Active control of combustion oscillations in a lean premixed combustor by secondary fuel injection

S. Tachibana*, L. Zimmer**, Y. Kurosawa* and K. Suzuki*

J. Shinjo**, Y. Mizobuchi** and S. Ogawa**

* : *Aeroengine Testing Technology Center, Japan Aerospace Exploration Agency*

** : *Information Technology Center, Japan Aerospace Exploration Agency*

7-44-1 Jindaiji-Higashi, Chofu, Tokyo 182-8522, Japan

E-mail: tachibana.shigeru@jaxa.jp

Abstract

Natural modes of combustion oscillation of a methane-air lean premixed combustor were investigated and open/closed loop controls were carried out by means of secondary fuel injections. The premixed flame was sustained by an axial vane swirler. Central part of the swirler was endowed a function as a secondary fuel injection nozzle. From the mode analysis of the pressure oscillations, it was revealed that the dominant mode shows transition from acoustic modes of the mixing chamber to that of the combustion chamber as the equivalence ratio increases. Strong pressure oscillations occurred in the intermediate range, $1790K<T_{ad}<1880K$ ($0.50<\phi<0.55$) , where the two dominant modes are competing. Open loop controls by secondary fuel injection in constant flow rates were applied on the condition of total equivalence ratio of 0.50, T_{in} = 700K and V_{swl} =90m/s. The results showed sensitivity to the injection amount and location. It indicates that the flame base is very sensitive to the additional fuel distribution. A similar discussion was made on NOx emissions also. Finally, a closed loop control was performed by implementing a mixed H^2/H^∞controller. An obvious effect of the closed loop control on suppression of pressure oscillations was found without loosing an advantage for low NOx emissions.

Introduction

Lean premixed (LP) combustion has a great advantage to reduce NOx emission without loss of combustion efficiency by controlling equivalence ratio that determines flame temperature to be in a suitable range. Thus it has attracted much attention from many researchers and developers on gas-turbine combustors. One main drawback of LP combustors is that it has a susceptibility to perturbations of the flow. It suffers from combustion instabilities like combustion oscillation, lean blow out and flash back. Among those, combustion oscillation is considered as a most problematic factor since it may lead to a sudden destruction or a cut-down of lifetime of an engine. To overcome the difficulties, passive controls have been widely adopted to the development of gas turbine combustors. In recent days, from the point of view of adaptive flexibility of the control, active control has begun to attract attention.

Combustion oscillations can be considered as a resultant phenomenon of strong coupling between the variations of pressure and heat-release rate. Thus many approaches have been performed by the idea based on thermo-acoustic theory. The purpose of active control of combustion is to break up the in-phase coupling. There exist several methods of actuations to achieve the purpose; for instance, loud speakers, adjustment of main fuel/air flow rates and secondary fuel/air injections. Among those, secondary fuel injections can be considered as a very promising choice for several reasons. One reason is related to the structure of the recent burners. Most recent burners consist of main and pilot burners. The role of the pilot is to enhance the capability for flame holding and/or ignitions. The pilot injector can be used as the actuator for active control. The other advantage comes from the flexibility of the injection location. The distribution of heat-release rate is closely linked with the flame position. The flame position is determined by the flame holding mechanism and will change for each combustor or operating conditions. Thus the location of actuation is an important issue to achieve an effective control. The method of secondary fuel injection has an advantage for the degrees of freedom of the locations.

There have been several works on active control by secondary fuel injection in recent days[1)-8)]. Lee et al.[1)] investigated the effects of injection locations on control effectiveness and reported that the effectiveness is strongly dependent on the location. In their case, 0 degree injection from the central hub showed the best performance on suppression of pressure levels. One main objective of their work was laid on the diagnostics of the effectiveness by applying optical measurements coupled with pressure measurements[1)-3)]. From phase-locked

chemiluminescence imaging, they proposed several useful methods to get effective injection locations or timing. Another important aspect of the actuation by secondary fuel injection is its effect on gas emissions, like NOx. Choi et al.[4] applied open loop controls by 45 degree-secondary fuel injection to combustion oscillations occurring in a swirl stabilized methane-air premixed combustor and investigated effectiveness on pressure levels, noise levels and NOx emissions. It was reported that both of the two levels and NOx emission were simultaneously suppressed in a range of operating condition. The suppression mechanism is reported in ref.5). In their case, combustion oscillations occurred for relatively higher load conditions, i.e. higher equivalence ratio. It may be due to the inlet temperature condition without preheating. Those results encourage ones to see the effects of secondary fuel injections on the combustion oscillation occurring in a fuel lean condition near the point of lean blow out (LBO).

In previous works at JAXA[6)-8)], the effects of angles and locations of secondary fuel injection on pressure levels and gas emissions have been investigated both for fuel rich and lean conditions. In this work, natural modes of combustion oscillation of the methane-air lean premixed combustor were investigated over the wide range of operating condition. Open and closed loop controls by secondary fuel injection with 30 degree angle were applied to the combustion oscillation occurring in a lean condition. The effects of the controls on the pressure levels and NOx/CO emissions were discussed in detail.

Experimental setup

Fig.1 shows the schematic of the combustion test rig. The rig is composed of an air supply system, an electric heater, a fuel-air mixing chamber and a combustion chamber. Dimensions of the parts are described in the figure. The combustion chamber has a length of 630mm with 100*100mm^2 rectangular cross-section. The upstream part of the chamber (210mm) is surrounded by four quartz glass windows so as to get optical information like chemiluminescence. The rest of the chamber is surrounded by four water-cooled stainless plates. The main fuel injector is placed at 260mm upstream from the inlet of the combustion chamber. The main fuel and air is supposed to be well mixed in space at the inlet. Methane was used as both for main and secondary fuels. The main premixed flame is sustained by an axial vane swirler. The design of the swirler is shown in Fig.2. The outer and inner diameters of the swirler are 50 and 20 mm respectively. It consists of 12 blades with an angle of 45 degree and installed with a receding distance of 20 mm from the inlet of the combustion chamber. Central (hub) part of the swirler is endowed a function as a secondary fuel injection nozzle. The nozzle is replaceable so that one can change the injection location easily. Several types of nozzles were examined in previous works[7),8)] and the nozzle with 30 degree injection angle was found most effective and chosen to apply in this work. The design of the nozzle is shown in Fig.2 also. The number of the orifices is 12 with a diameter of 0.8mm. The design concept of the nozzle is based on the idea that the stability of the global flame is greatly governed by the stability of the flame base. In this case, near-downstream region from the central hub is considered as the position of the flame base. While pressure antinode stays at the closed end, i.e., the inlet of the combustion chamber. This means that the region of the flame base is the most probable position that suffers from the strong coupling between pressure and heat release rate variations. Thus the secondary injection from the position has a possibility to give great effects on the flame stability.

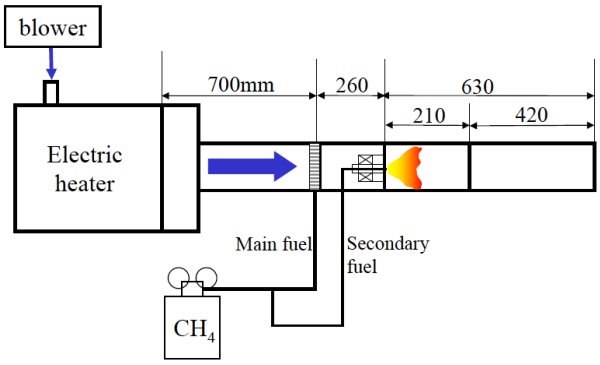

Fig.1 Schematic of the combustion test rig

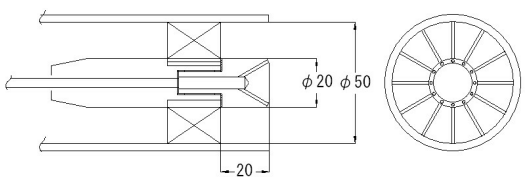

Fig.2 Design of the axial-vane swirler with secondary fuel injection orifices.

Measurement system

Schematic of the measurement system is shown in Fig.3. The system consists of 4 pressure transducers (Kulite Semiconductor Products, Inc., Model XTL-190-15G) for the measurements of pressure variations, an ICCD camera (Princeton Instruments 576G/1, 576*384 pixels with a UV-Nikkor 105mm/f4.5 lens) and a gas analyzer (Horiba, MEXA-9110, NO, NOx, CO, CO2, THC, O2). The semi-infinite tube technique[9] was applied for all the pressure measurements. Signals from the pressure transducers were acquired simultaneously through a multi-channel data acquisition system (ONO SOKKI, DS-200, Graduo). Typical sampling frequency was 25.6kHz for each channel. Pressure signals from the transducer at x=10mm was used as the triggering signal for phase-locked OH* image measurement by ICCD. In the measurement, the frequency of the peak SPL was detected first and a band pass filter centered on the frequency was applied on the raw pressure signal. The triggering position was set on the filtered signal as the zero-crossing point with a positive slope. Then the phase-locked measurement took place by setting phase delays from the trigger. For the conditions of ICCD, the gate width was set to 50 micro sec, the gain to 100%, the aperture to 4.5 and 30 images were accumulated for each phase.

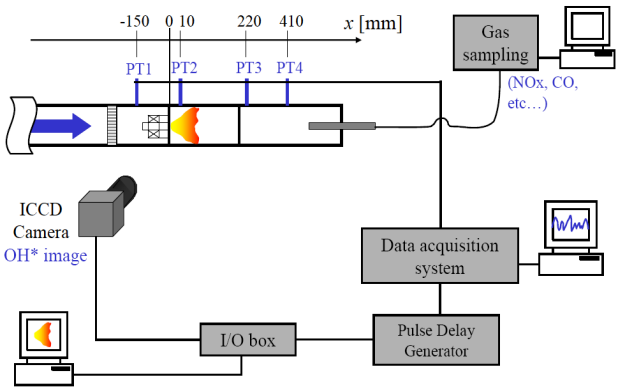

Fig.3 Schematic of the measurement system

Control system

Configuration of the control system is shown in Fig.4. Pressure transducer was used as a sensor. In the case of closed loop control, a MOOG D633 high bandwidth electromagnetic directly driven proportional valve was implemented. The valve is known for the capability of high bandwidth up to 400Hz[10)-12)]. To improve the fuel modulation capability by the valve, a plenum chamber was inserted into the fuel line just before the valve in the similar way to ref.10). A mixed H^2/H^∞controller was applied to get both effectiveness on the exciting frequency and robustness over the whole frequency domain simultaneously. The detailed description on the design of the controller can be found in ref.14).

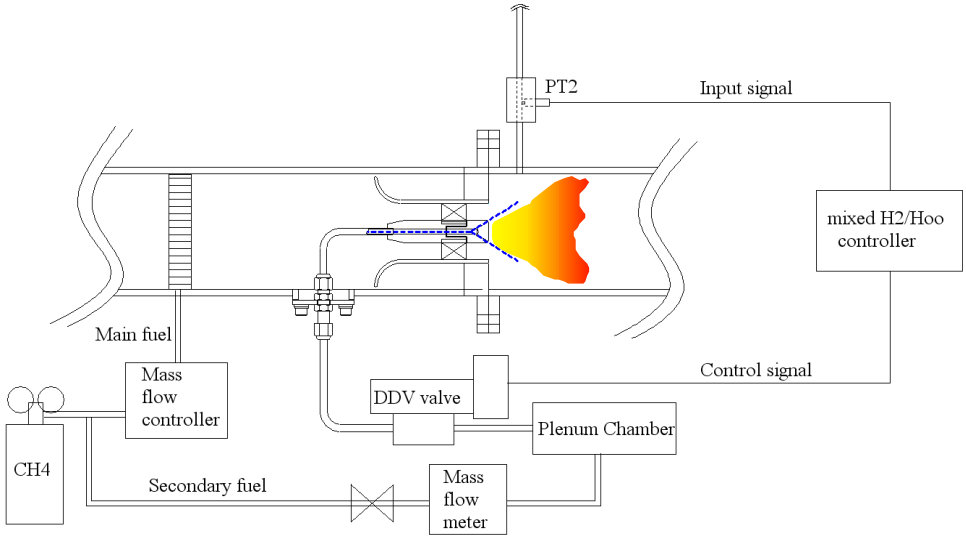

Fig.4 Control system configuration

CFD configuration

To understand combustion dynamics in a comprehensive way to implement appropriate combustion control, numerical simulation was also carried out based on Large-Eddy Simulation (LES) and the flamelet model. The objective of this approach was to investigate the mechanisms of combustion oscillation and to obtain implications for combustion control using secondary fuel injection.

The numerical method used here was a compressible finite volume method to capture acoustic wave propagation inside the combustor. Grid scale phenomena were solved directly on the numerical mesh of the order of 10 million points, and sub-grid scale structures were given by the Smagorinsky sub-grid scale model. Because the premixed flame thickness is relatively thin compared to the combustor size, the flame was modeled as a discontinuity surface between burned and unburned gases. The propagation of the flame was described by the well-known G-equation.

The combustor configuration was the same as the experimental one. The calculation domain included swirler inlet, combustor and downstream region. The flow conditions were the temperature of 700K, inlet velocity of 90m/s and equivalence ratio of 0.5.

Results and discussion

Natural modes of the combustor

Natural modes of the combustor were investigated for the condition of T_{in} = 700K and Q_{air}=78 g/s that give a nominal velocity of the swirl area V_{swl} =90m/s. In this case, no secondary fuel was injected. The experiment was pursued by increasing fuel flow rate, i.e. equivalence ratio. Fig.5 shows the stability curve. Square and triangle symbols represent respectively the peak value of sound pressure levels (SPL) and the frequency of the peak. Lean blow out occurred in between ϕ=0.420-0.425(T_{ad}=1638-1642K). The peak SPL shows clear transition to the higher levels, SPL~160-170, around T_{ad}=1700K (ϕ=0.45) and decreases rapidly in between T_{ad}=1876-1893K (ϕ=0.55-0.56). On the frequency domain, it seems that the whole domain can be divided into three. For leaner conditions, T_{ad}=1660-1771K (ϕ=0.43-0.49), the frequency shows a flat distribution, in other words, no dependency on equivalence ratio. For the intermediate range, T_{ad}=1788-1876K (ϕ=0.50-0.55) , the frequency increases with a relatively steep slope as equivalence ratio goes up. Then for richer conditions, T_{ad}=1893K-(ϕ=0.56-), it still shows a positive but moderate slope. The emission properties of NOx and CO in the same operating range are shown in Fig.6. By comparing with Fig.5, one can find that the strong oscillation occurs in the range where both emissions stay at lower levels. This is a typical problem of lean premixed combustors.

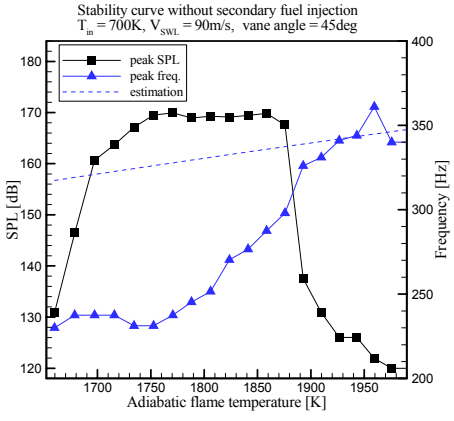

Fig.5 Stability curve vs flame temperature

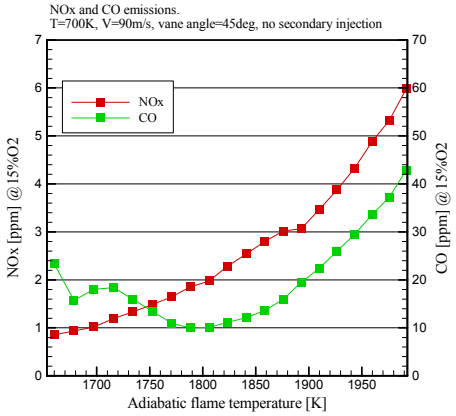

Fig.6 Emission properties of NOx and CO

Fig.7(a)-(d) show typical distributions of power spectrum density (PSD) for four conditions, i.e., T_{ad}=1697, 1788, 1824 and 1893 K (ϕ=0.45, 0.50, 0.52 and 0.56) respectively. In Fig.7(a), the spectra for mixing chamber (x=-150mm) and combustion chamber (x=10, 220mm) show similar tendency. The first peak appears around 240Hz and second and third harmonics appear next in descending order. Only an exception can be found for the third peak around 830Hz at x=10mm. It may be due to the effect of 3/4 acoustic mode of combustion chamber. In

this case, the driving mode can be considered to be the acoustic mode of the mixing chamber with fixed end boundaries. Thus, the peaks are in the order of 1/2, 2/2, etc. The flat distribution (see Fig.5) also supports the explanation since the velocity of sound does not change for unburnt gas. In Fig.7(b), the peaks show higher values than in Fig.7(a), but the tendency is almost the same. On the other hand, in Fig.7(c), the spectra show different trends. The spectrum of the mixing chamber keeps the descending order but that of the combustion chamber (x=10mm) does not. Alternatively, the modes corresponding to the 1/4 and 3/4 of the combustion chamber seem to appear. Thus this domain seems to be driven by a mixing mode between the mixing chamber and the combustion chamber. As can be seen from Fig.5, this domain is corresponding to the most unstable regime. Finally, in Fig.7(d), one can only see the mode of combustion chamber. The dashed line in Fig.5 is the estimate for the 1/4 mode of combustion chamber calculated by adiabatic temperature on each condition. The slope of the plots in this domain agrees well with the estimated line. One can summarize that the dominant mode shows transition from the acoustic mode of the mixing chamber to that of the combustion chamber as the equivalence ratio increases and strong pressure oscillations occur in the range where the two dominant modes are competing.

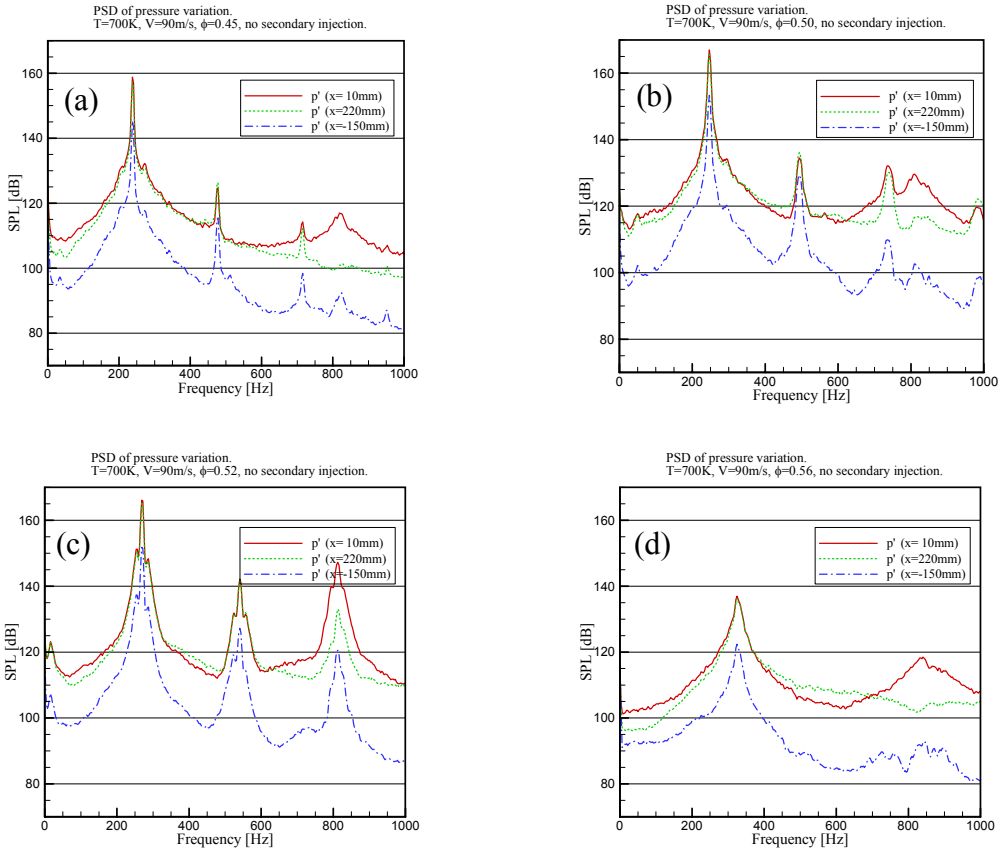

Fig.7 Power spectrum densities of pressure variation. Tad= (a)1697 K, (b) 1788 K, (c) 1824 K, (d) 1893 K.

CFD analysis of the natural mode of the combustor

CFD results are also presented to obtain insights on the combustion dynamics in the combustor. Fig.8 shows the time-averaged velocity field. The upper part of the combustor from the dump plane is shown. The incoming flow is swirled and expands at the dump plane. Due to the swirling motion, corner and central recirculation zones are created. The central recirculation zone pushes hot burned gas upstream to stabilize the flame at the swirler exit.

Inside the combustor, several pressure oscillation modes are present. These oscillations determine the flame behavior and dynamics. Fig.9 shows traces of global heat release and flame surface area in one cycle of combustion oscillation inside the combustor. The basic frequency is observed around 300Hz, which corresponds to the acoustic quarter-wave mode.

Pressure waves inside the combustor cause velocity fluctuations, leading to periodic vortex shedding from the

dump plane. Fig.10 shows instantaneous snapshots of vorticity magnitude and the flame shape on the center plane of the combustor in one cycle of oscillation. The phase information was calculated by the delay time from the zero point of pressure variation sampled at the similar position with the PT2 in experiment (see Fig.3). In the images, several vortical structures are seen and they often exist near the flame surface. When these vortices come close to the flame surface, the flame shape and position can be affected. This leads to fluctuations in global heat release rate because the flame surface area is changed by vortical motions, as can be seen in Fig.9. Due to high viscosity in the hot burned gas side, these structures are likely to be attenuated as they go downstream.

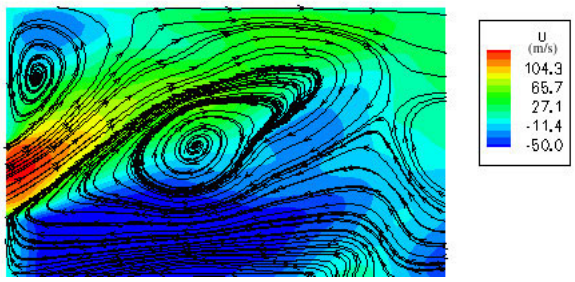

Fig.8 Time-averaged velocity field
Tin=700K, Vswl=90m/s, ϕ=0.50

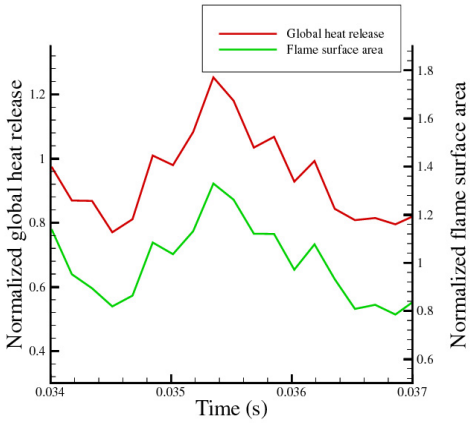

Fig.9 Global heat release and flame surface area evolution in one cycle

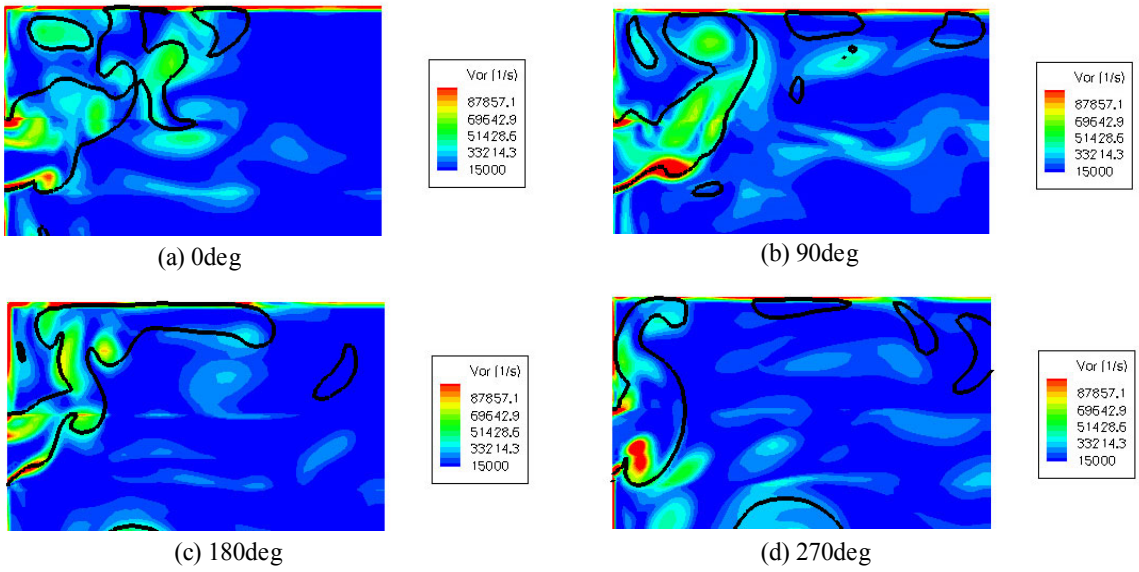

(a) 0deg (b) 90deg

(c) 180deg (d) 270deg

Fig.10 Evolution of vorticity magnitude and flame (a) 0deg, (b) 90deg, (c) 180deg, (d) 270deg from zero point

Thermal expansion by combustion increases local flow velocity at the flame surface. The wrinkled flame shape causes flow acceleration in various directions. The time-averaged axial velocity fluctuation magnitude is shown in Fig.11. The fluctuation magnitude is strong where the mean flame is present and this can be mostly attributed to thermal expansion. The velocity fluctuation may lead to local pressure fluctuation. Then the pressure fluctuation may be formed into resonant modes of the combustor. Resonant acoustic frequencies can be determined by the combustor configuration. For example, for an open-end combustor, the outer boundary is usually a pressure node.

This feedback mechanism from heat release fluctuation to pressure fluctuation can be explained by the acoustic energy balance, or the Rayleigh index. If the index is positive, the combustion energy is fed into the acoustic energy. If the index is negative, it works in the opposite way. Fig.12 shows the local Rayleigh index distribution. The index is mostly positive in the flame region, thus this feedback mechanism is observed. Making this unstable flow field stable, the heat release field should be changed by secondary fuel injection to reduce the coupling.

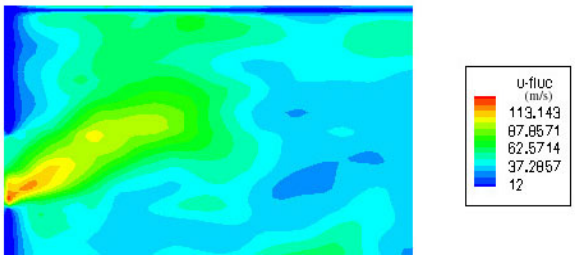

Fig.11 Time-averaged axial velocity fluctuation

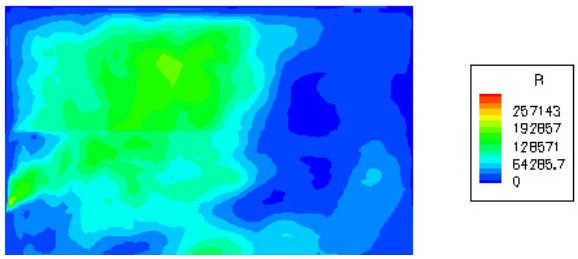

Fig.12 Local Rayleigh index distribution

Open loop controls by the secondary fuel injection at constant flow rates

To investigate the effects of the open loop control by secondary fuel injection, a series of experiments were conducted for the 30 degree injection nozzle (see Fig.2). As a typical case for strong oscillations, a total equivalence ratio of 0.50 was chosen for the target. With the total equivalence ratio fixed at 0.50, percentage of the flow rate of secondary fuel against total fuel was changed from 2 to 10 %. For each percentage, the secondary fuel was injected at a constant flow rate.

In Fig.13 show the effect of secondary fuel injection on peak pressure levels and NOx emissions. The pressure levels were normalized by the value in the case of no injection. The values for NOx emission are corresponding to the averaged values over 8 locations. For the sampling locations, x position was fixed at -50mm from the exit of the combustion chamber and y and z positions were changed by a traversing system. 8 positions, y=z=0, 5, 10, 15, 20, 25, 30, 35mm, were measured to get a representative value of the condition. As can be seen easily from the rectangular plots in Fig.13, the secondary fuel injection effectively works on the reduction of pressure levels. More than 20dB reduction can be achieved with 4% or more of the injection. The secondary fuel injected from 12 orifices seemed to produce 12 jet diffusion flames in the region of flame base. The existence of diffusion flames was identified by the appearance of C2* band peaks in the spectrum of chemiluminescence emission and is reported in ref.13). The small diffusion flames will fix the distribution of heat-release rate in the region and suppress spatial and temporal variations of the distribution. The stabilization of flame base makes the flame response against pressure variation small. This process can be considered as the decoupling mechanism of the thermo-acoustic instability and called “re-distribution of heat-release rate”. On the other hand, NOx emission shows linear increment as the fuel percentage increases. It indicates also that the secondary flames can be considered as diffusion flames.

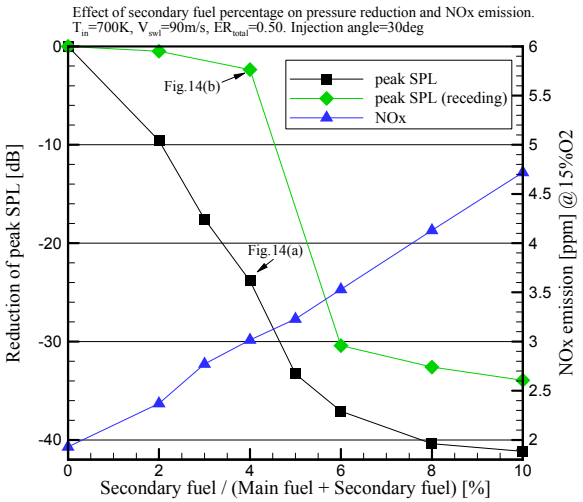

Fig.13 Effects of secondary fuel injection on pressure levels and NOx emission

In order to show sensitivity to injection locations, the peak pressure levels for another nozzle are shown also in Fig.13 as diamond symbols. In this case, injection orifices were placed at a receding position, 5mm upstream from the former injection location. Only 2.4dB reduction can be achieved by 4% injection in contrast with the

result of the former nozzle that showed 23.8dB reduction. To see the positions of the source of instability, 2-dimensional Pseudo-Rayleigh Index (PRI) maps were calculated. In order to derive the maps, three assumptions were adopted in the similar way to Lee et al[1]. One is that the OH* chemiluminescence intensity is proportional to the heat release rate of the flame. The second is that the flame is axisymmetric thus the Abel inversion transform can be applied to the raw OH* image so as to reduce the line-of-sight information to 2-dimensional cut distribution. The third is that the pressure distribution in the measured area can be considered uniform in space. Then the PRI map, *R(x,y)*, can be calculated from the measured pressure and Abel inversion of the OH* distribution as follows:

$$R(x,y) \sim \frac{1}{\tau}\int_{\tau} p'(t)\cdot I'_{OH^*}(t,x,y)dt$$

where τ is the time period for one cycle of the oscillation, *p'* is the variation of pressure and I'_{OH^*} is the variation of Abel-inverted OH* chemiluminescence intensity. Fig.14(a) and (b) show PRI maps for the nozzles of 30 degree without and with the receding distance respectively. Total equivalence ratio was set to 0.50 and the fuel percentages are 4% for both cases. Only the region beyond a threshold (in this case the value of -3) is displayed. Sometimes there exists a region with large negative values that indicates, in principle, strong attenuation of the instability. However if one considers the flame stabilization mechanism, the region will be filled mostly by burnt gas and thus the strong negative may be an apparent result due to the limitation of the process. If one focuses the discussion on the distribution of the higher positive values, one could deal with the distribution in a qualitative sense. Those figures represent typical examples of (a) an effective case and (b) a non-effective case (see indications in Fig.13 also). In the effective case, Fig14(a), there can be seen no clear distribution over the whole region, whereas in the non-effective case, there can be found two regions that show strong magnitude, in other words, strong coupling between pressure and heat-release rate. The locations are corresponding to near-field from the nozzle and near the chamber wall. Those results indicate that there exists sensitivity to injection locations and the location has to be determined thoughtfully.

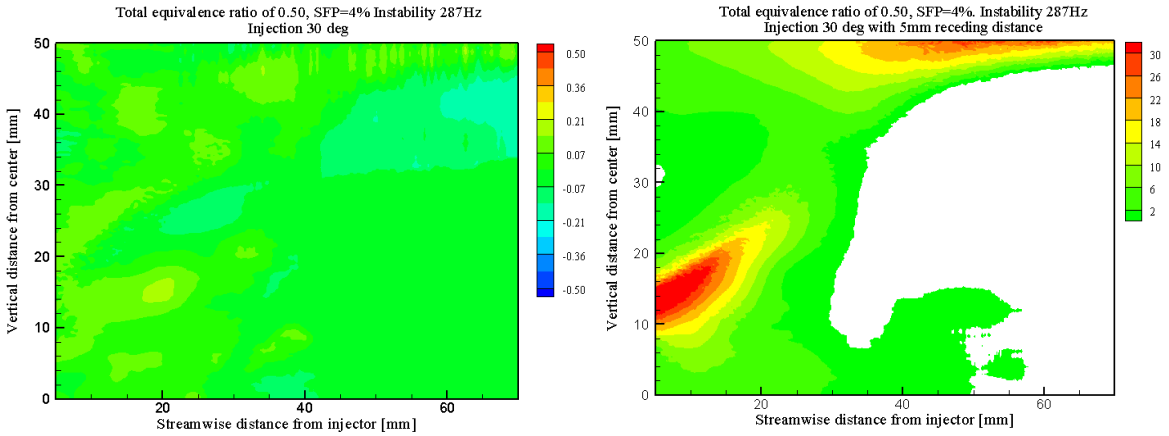

(a) (b)

Fig.14 Pseudo-Rayleigh index maps. Total equivalence ratio of 0.50 and secondary fuel percentage of 4%. (a) Effective case (Injection of 30 deg), (b) Non-effective case (Injection of 30 deg with a receding distance of 5mm)

Closed loop control by the mixed H^2/H^∞ controller

Finally, a closed loop control by the mixed H^2/H^∞ controller was conducted on a lean unstable condition. In this case, the control system shown in Fig.4 is totally working. As a typical case for strong oscillations, a total equivalence ratio of 0.50 was chosen for the target again. By adjusting source pressure of the secondary fuel, mean flow rate of injection was set to 3% of the total fuel. The design concept of the controller, system identification procedure and the simulation results are described precisely in ref.14). Only the results of the pressure levels and emission are shown here. In Fig.15 show the spectra for non-controlled, open-loop controlled and closed-loop controlled cases. Non-controlled means that no secondary fuel injection is applied and the spectrum is the same as shown in Fig.7(b). By the open loop control, the peak value shows 17dB reduction. The

peak frequency shifts from 250 to 280Hz also. This is due to the effect of heat-release re-distribution as described in previous section. When the closed loop was applied, peak level shows 10dB further reduction. This is purely the effect of the designed controller. The peak frequency shifts toward the higher side again, from 280 to 290Hz. In this case, the spectrum shows local maximum and minimum around 164 and 178 Hz respectively. This trend was not observed for other cases. The results of the control simulation showed similar trend[14]. Thus it can be considered as a feature of the controller. The effects of the controls are summarized in Table.1. Increments of gas emissions due to secondary fuel injection were within 1 and 3.5 ppm for NOx and CO respectively. Those changes can be considered small compare to the drastic reductions in pressure levels. Furthermore, one can find that the closed loop control gives 10dB additional reduction in pressure levels over open loop control without influencing the gas emission properties. Consequently, the closed loop control with a small amount of secondary fuel injections can be considered as a promising candidate for the active control of practical gas turbine combustors.

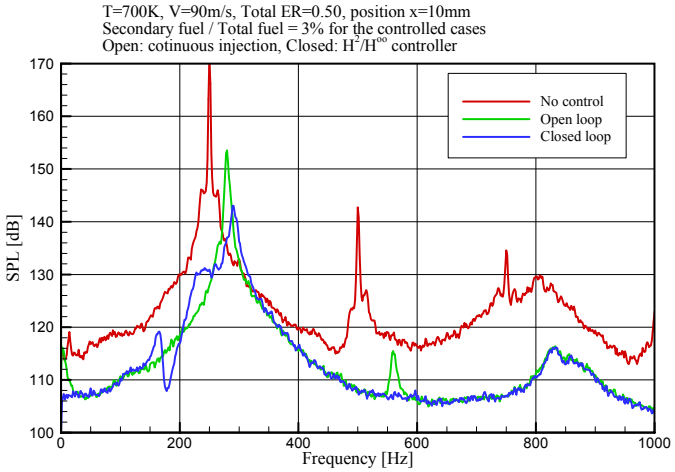

Fig.15 Effects of controls on pressure levels

Table.1 Comparison of the effects of open/closed controls

Control	Peak SPL [dB]	Reduction[dB]	NOx [ppm] @15%O2	CO [ppm] @15%O2
No control	171.0	---	1.93	2.98
Open loop	153.5	17.4	2.77	6.27
Closed loop	143.0	27.9	2.68	6.20

Conclusions

Natural modes of a model premixed combustor were investigated by increasing equivalence ratio from 0.43 to 0.62 on the fixed conditions of T_{in} = 700K and V_{swl} =90m/s. The dominant mode showed transition from the acoustic mode of the mixing chamber to that of the combustion chamber as the flame temperature, or equivalence ratio, increases. Strong pressure oscillations occurred in the intermediate range, T_{ad}=1788-1876 K (ϕ=0.50~0.55), where the two dominant modes are competing.

Open loop controls actuated by the secondary fuel injection of constant flow rates were applied for the condition of total equivalence ratio of 0.50. The secondary fuel injection effectively worked on the reduction of pressure levels. More than 20dB reduction can be achieved with 4% or more of the injection. NOx emission showed linear increment as the fuel percentage increases.

A closed loop control by the mixed H^2/H^∞controller was performed on the condition of total equivalence ratio of 0.50. Mean value of the secondary fuel percentage was set to 3%. An obvious effect of the closed loop on suppression of pressure oscillations, compared with that of open loop, was found without loosing an advantage for low NOx emissions.

Acknowledgement

The authors are pleased to acknowledge the support of the Center for Smart Control of Turbulence, the Ministry of Education, Culture, Sports, Science and Technology of Japan.

Nomenclature

ϕ	[-]	Equivalence ratio
ϕ_{total}	[-]	Total equivalence ratio
I_{OH*}	[a.u.]	Abel inverted distribution of OH* intensity
T_{in}	[K]	Inlet air temperature
Q_{air}	[g/s]	Mass flow rate of air
V_{swl}	[m/s]	Bulk mean velocity for the area of the swirler

References

1) Lee, J.G., Kim, K., and Santavicca, D.A., *Proc. Combust. Inst.* **28**:739-746 (2000)
2) Kim, K., Lee, J. G. and Santavicca, D. A., *AIAA paper*, *AIAA 2002-4024* (2002)
3) Lee, J. and Santavicca, D. A., *Journal of Propulsion and Power*, **1**9:735-750 (2003).
4) Choi, G. M., Tanahashi, M. and Miyauchi, T., *Proc. Combust. Inst.* **30**, 1807-1814. (2004)
5) Tanahashi, M., Kikuta, S., Shiwaku, N., Kato, S., Inoue, S., Taka, S. and Miyauchi, T., "Turbulent Combustion Controls based on Local Flame Structure", *Proc. The 6th Sym. Smart Control of Turbulence* (2005)
6) Tachibana, S., Zimmer, L., Yamamoto, T., Kurosawa, Y., Yoshida, S. and Suzuki, K., *Proc. The 5th Sym. Smart Control of Turbulence*, 175-183. (2004)
7) Tachibana, S., Zimmer, L., Kurosawa, Y. and Suzuki, K., 42nd Symposium on Combustion, Gifu, 1-3 December (2004) in Japanese.
8) Tachibana, S., Zimmer, L., Kurosawa, Y. and Suzuki, K., *Asian Joint Conf. on Propulsion and Power, Fukuoka*, 27-29th Jan. (2005)
9) Englund D. R., Richards W.B., "The infinite line pressure probe", *Proc. of the 30th intern'l instrumentation symp.*, pp.115-124 (1984)
10) Hantschk, C., Hermann, J. And Vortmeyer, D., *Proc. Combust. Inst.* **26**, 2835-2841.(1996)
11) Hermann, J., Orthmann, A., Hoffmann, S. and Berenbrink, P., *Proc. Of the NATO/RTO Symp. On Active Control Technology*, RTO, Braunschweig, Germany (2000)
12) Bernier, D., Ducruix, S., Lacas, F., Candel, S., Robart, N. And Poinsot, T., *Combustion Science and Technology*, 175: 993-1013(2003)
13) Zimmer, L., Tachibana, S., Tanahashi, M., Shimura, M. and Miyauchi, T., "Sensors for active control of combustion", *Proc. The 6th Sym. Smart Control of Turbulence* (2005)
14) Sato, H., Hayashi, K., Ikame, M., Kishi, T., Harumi, K., Tachibana, S., Zimmer, L. and Ogawa, S., "Design of Active Control System for Combustion Instability Using Mixed H^2/H^∞ Algorithm", *Proc. The 6th Sym. Smart Control of Turbulence* (2005)